

Cu NQR Studies of the Superconductors $\text{YBa}_2\text{Cu}_3\text{O}_x$ and $\text{YBa}_2\text{Cu}_4\text{O}_8$

D. Brinkmann

Physik-Institut, University of Zürich, Zürich, Switzerland

Z. Naturforsch. **45a**, 393–400 (1990); received August 22, 1989

The paper reviews some copper NQR studies in the superconductors $\text{YBa}_2\text{Cu}_3\text{O}_x$ and $\text{YBa}_2\text{Cu}_4\text{O}_8$ performed at the University of Zürich. The following topics are discussed: the temperature and pressure dependence of the NQR frequencies; relation between linewidths and oxygen deficiency; the determination of the electric field gradients (EFG) and Knight shifts at the copper sites; discussion of some calculations of the EFG tensors; measurements of the various relaxation times in all phases. The results obtained in both structures are compared; possible interpretations are discussed.

1. Introduction

Magnetic resonance played an important role in understanding superconductivity when the Bardeen-Cooper-Schrieffer theory provided the first microscopic explanation of this extraordinary state of matter [1]. Thus it was natural that the NMR/NQR community soon after the discovery of the new high- T_c superconductors began to devote much activity to these new materials. The power of NMR and NQR lies in the fact that these methods can provide information on static and dynamic properties on an atomic scale [2].

In this paper we will review several copper NQR studies our NMR group at the Physik-Institut of the University of Zürich has performed in high- T_c superconductors. We will refer to published data and to some papers being in press or submitted for publication. We will deal with two members of the Y-Ba-Cu-O family: the “1-2-3-X” structure $\text{YBa}_2\text{Cu}_3\text{O}_x$ (where x has values close to 6 and 7) and the “1-2-4” structure $\text{YBa}_2\text{Cu}_4\text{O}_8$ which recently has been synthesized as bulk material by the group of E. Kaldis [3]. Comparison of results obtained in related structures such as “1-2-3-7” (with $T_c=92$ K) and “1-2-4” ($T_c=81$ K) may lead to new insights into the microscopic behavior of these materials.

We will report on (1) the temperature and pressure dependence of the copper NQR frequencies, (2) the

relation between linewidths and oxygen deficiency, (3) the determination of the electric field gradients (EFG) and Knight shifts present at the copper sites, (4) discussion of some calculations of the EFG tensors, (5) measurements of the various relaxation times in all phases. This information serves as essential input for testing models or constructing theories to explain the mechanism of superconductivity.

2. Details on Material and Experiments

We briefly summarize some pertinent structural information about the compounds we have investigated. We have studied the two “end” members of the “1-2-3” material: the superconductor with $x \approx 7$ and $T_c=92$ K and the antiferromagnetic semiconductor ($x \approx 6$) with $T_N=418$ K. Both compounds, which have an oxygen-deficient perovskite-like structure contain two inequivalent copper sites: the chain forming Cu1 sites and the planar Cu2 sites. The latter are five-coordinated by an apically elongated rhombic pyramid of oxygen ions. In the “1-2-3-7” orthorhombic structure the Cu1 ion is at the center of an oxygen rhombus-like square, while in the tetragonal “1-2-3-6” structure the nearest neighbors of Cu1 are the two oxygen O1 on the c axis.

The orthorhombic unit cell of the “1-2-4” structure [4, 5] can be considered as two “1-2-3-7” unit cells joined chain-to-chain with the second cell displaced by $b/2$ along the b axis. Thus, instead of the single Cu–O chains of “1-2-3-7”, the “1-2-4” structure contains double Cu–O chains which form an edge-sharing, square-planar network.

* Presented at the Xth International Symposium on Nuclear Quadrupole Resonance Spectroscopy, Takayama, Japan, August 22–26, 1989.

Reprint requests to Prof. Dr. D. Brinkmann, Physik-Institut, Universität Zürich, Schönberggasse 9, CH-8001 Zürich.

0932-0784 / 90 / 0300-0393 \$ 01.30/0. – Please order a reprint rather than making your own copy.



Dieses Werk wurde im Jahr 2013 vom Verlag Zeitschrift für Naturforschung in Zusammenarbeit mit der Max-Planck-Gesellschaft zur Förderung der Wissenschaften e.V. digitalisiert und unter folgender Lizenz veröffentlicht: Creative Commons Namensnennung-Keine Bearbeitung 3.0 Deutschland Lizenz.

Zum 01.01.2015 ist eine Anpassung der Lizenzbedingungen (Entfall der Creative Commons Lizenzbedingung „Keine Bearbeitung“) beabsichtigt, um eine Nachnutzung auch im Rahmen zukünftiger wissenschaftlicher Nutzungsformen zu ermöglichen.

This work has been digitalized and published in 2013 by Verlag Zeitschrift für Naturforschung in cooperation with the Max Planck Society for the Advancement of Science under a Creative Commons Attribution-NoDerivs 3.0 Germany License.

On 01.01.2015 it is planned to change the License Conditions (the removal of the Creative Commons License condition “no derivative works”). This is to allow reuse in the area of future scientific usage.

The NQR and NMR experiments to be described were carried out using pulsed spectrometers. The NQR measurements were done in zero magnetic field, the NMR experiments in superconducting magnets of field strengths around 5 T. NMR spectra were obtained by scanning the frequency in discrete steps and by sweeping the static field by ± 0.08 T. All signals were obtained by the spin-echo technique either by integrating the echo signal (NMR) or by Fourier transformation of the whole echo (narrow NQR signals). Very broad NQR signals were detected pointwise. The spin-lattice relaxation times T_1 were measured on the NQR echo using the $\pi - t_w - (\pi/2) - \pi$ pulse sequence, where the π pulse inverts the population and t_w is the “waiting” time.

3. Linewidth and Temperature and Pressure Dependence of NQR Signals

The copper NQR experiments in both “1-2-3-7” [6, 7, 8] and “1-2-4” [9] yield four signals because there are two Cu sites and two copper isotopes ^{63}Cu and ^{65}Cu . The NQR frequency ν_Q of these signals is related to the principal components V_{ii} of the EFG tensor present at the Cu site by

$$\nu_Q = \frac{eQV_{zz}}{2h} \sqrt{1 + \frac{1}{3}\eta^2}. \quad (1)$$

Here, η is the asymmetry parameter defined as $\eta = (V_{xx} - V_{yy})/V_{zz}$, where $|V_{zz}| \geq |V_{yy}| \geq |V_{xx}|$, and eQ is the nuclear electric quadrupole moment. Thus the ratio of the NQR frequencies of the two isotopes is equal to the ratio of their quadrupole moments (1.081). This has been confirmed experimentally for both Cu sites in “1-2-3-7” and “1-2-4” and for Cu1 in “1-2-3-6”. This proves that no internal magnetic field due to any type of magnetic ordering is present at these Cu sites (in the temperature range we have studied); such a field would split or shift the NQR lines. [The Cu2 signal in “1-2-3-6” which we have not studied is shifted due to antiferromagnetism.]

In order to understand the large linewidth $\Delta\nu$ of the Cu NQR signals we have measured $\Delta\nu$ in “1-2-3-X” for oxygen concentrations x ranging from about 6.940 to 6.983 with uncertainties of ± 0.001 [10]. Figure 1 shows that $\Delta\nu$ of the Cu1 signal increases linearly with oxygen deficiency $\delta = 7 - x$. Extrapolation of the data to $\delta = 0$ leaves a “rest” linewidth of about 40 kHz whose origin is due to other effects than oxygen de-

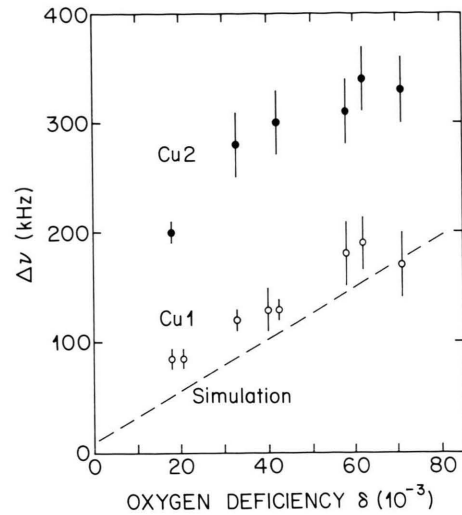


Fig. 1. Linewidth $\Delta\nu$ (“full width at half height”) of the ^{63}Cu NQR signals of both Cu sites in $\text{YBa}_2\text{Cu}_3\text{O}_{7-\delta}$ as a function of oxygen deficiency δ . The dashed line is the result of simulation discussed in the text (from [10]).

iciency, for instance crystal structure defects. The intrinsic linewidth arising from spin-spin relaxation is only about 10 kHz.

To our knowledge these are the smallest Cu NQR linewidths measured so far in powder samples of high- T_c superconductors; the improvement against earlier samples is considerable. For the Cu2 linewidth, the $\Delta\nu$ vs. δ dependence is less clear and more experimental data at small δ are required.

We have calculated the effect of the oxygen vacancies on $\Delta\nu$ by a computer simulation assuming a random distribution of oxygen vacancies on the chain 04 sublattice and using the point charge model [10]. The simulated $\Delta\nu$ increases linearly with δ (see Fig. 1) and is practically the same for Cu1 and Cu2. This result agrees quite well with the experimental data for the Cu1 signals. That the Cu2 signals are about twice as broad as the Cu1 signals may be traced back to the fact that an oxygen vacancy wipes out the contribution of its next-neighbor Cu1 nucleus to the Cu1 signal while the effect on the Cu2 – a charge redistribution around Cu2 neighbors – is less severe, leading to a detectable broadening of the signal.

In “1-2-4”, the linewidths at 350 K are about 60 kHz for Cu1 and 170 kHz for Cu2 [9]. They seem to be compatible with fully occupied oxygen sites, as seen in neutron diffraction [11].

We have measured the dependence of ν_Q on both temperature T and pressure P for various Cu sites and

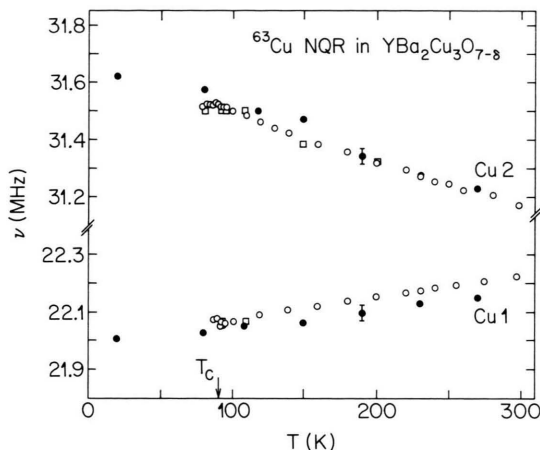
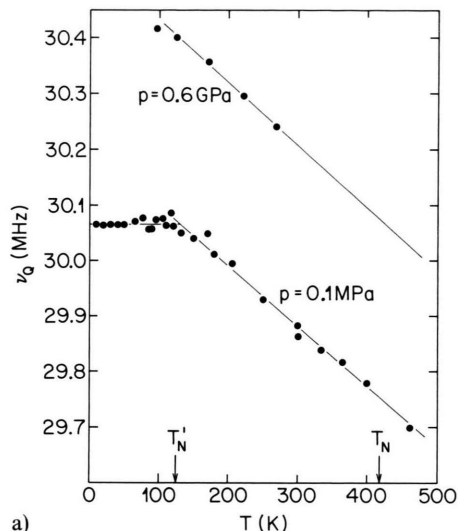


Fig. 2. Temperature dependence of Cu NQR frequencies in various $\text{YBa}_2\text{Cu}_3\text{O}_{7-\delta}$ samples. Different symbols distinguish slightly different values of δ (from [6, 12]).

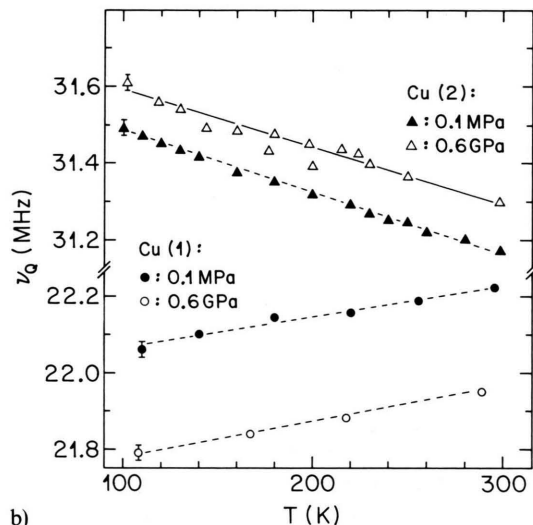
compounds. In “1-2-3-X” we have determined $\nu_Q(T)$ and $\nu_Q(P)$ for all sites except the Cu2 site in “1-2-3-6” [6, 7, 12, 13]; in “1-2-4” we have measured $\nu_Q(T)$ for both sites [9]. Figure 2 is a summary of $\nu_Q(T)$ data for various samples of “1-2-3-7” with slightly different oxygen content [6, 12]. A small dependence of ν_Q on oxygen content is present. However, we could not detect at T_c or other temperatures any indication for major structural changes, which should reveal themselves by abrupt variations of ν_Q . Riesemeier et al. [this conference] will report on changes of ν_Q at T_c .

In “1-2-4” the higher precision of the NQR frequencies allows to discern small changes of ν_Q with temperature [9], for instance around 200 K, where the derivative of $\nu_Q(\text{Cu}2)$ with respect to temperature changes its sign, or at 240 K, where Martin et al. (see [14]) have observed kinks in the resistance and Hall coefficient in thin-film samples. On the other hand, at and just below T_c we have not yet obtained any evidence for a structural phase transition. More experimental data are needed in this temperature range.

Figure 3 gives some examples for the temperature and pressure dependence of the NQR frequencies. The change of ν_Q with temperature and/or pressure depends on both site and structure. For instance, in “1-2-4” $\nu_Q(\text{Cu}1)$ increases monotonously with rising temperature [9] as in “1-2-3-7” (Fig. 3b), however at an overall rate which is lower. On the other hand, $\nu_Q(\text{Cu}2)$ in “1-2-4” exhibits a change of slope around 200 K and levels off above 550 K [9], i.e. in a temperature range that was not accessible in “1-2-3-7”.



a)



b)

Fig. 3. Temperature dependence of the NQR frequency ν_Q of ^{63}Cu for Cu1 site in $\text{YBa}_2\text{Cu}_3\text{O}_6$ (Fig. 3a) and Cu1 and Cu2 sites in $\text{YBa}_2\text{Cu}_3\text{O}_7$ (Fig. 3b) at two different pressures (from [13]).

Considering the pressure dependence of ν_Q in “1-2-3-7” (Fig. 3b) we note that pressure seems to “enhance” the effect of lowering the temperature; e.g. for Cu2 an increase of pressure shifts ν_Q to even higher values. The behavior of Cu2 is expected in the framework of a picture where compression of the crystal increases ν_Q ; for Cu1 this is not true. For the compounds we have studied, ν_Q at constant temperature always varies linearly with pressure (up to 0.6 GPa), however with rates differing in magnitude and sign.

By measuring separately both the temperature and pressure dependence of ν_Q it is possible to determine the phonon contribution to the temperature variation of ν_Q [15]. We assume that ν_Q depends on volume V and T in the following way:

$$\nu_Q = \nu_Q[V_{zz}(V), \eta(V), \xi^i(V, T)], \quad (2)$$

where ξ^i are the amplitudes of the lattice vibrations. Using thermodynamic relations one derives from (2) the expression

$$\left(\frac{\partial \nu}{\partial T}\right)_V = \left(\frac{\partial \nu}{\partial T}\right)_P - \frac{V_T}{V_P} \frac{\alpha}{\lambda} \left(\frac{\partial \nu}{\partial P}\right)_T, \quad (3)$$

where α and λ are the coefficients for volume expansion and isothermal compression, respectively, and V_T and V_P are the respective volumes. Using the experimental values $\nu_Q(T)$ and $\nu_Q(P)$, one calculates from (3) the phonon contribution $(\partial \nu / \partial T)_V$ to the temperature derivative of the NQR frequencies. For “1-2-3-7”, this contribution is negative in accord with simple models such as that of Bayer, and it is much larger for Cu1 than for Cu2, reflecting the large vibrations of the Cu1 oxygen neighbors.

4. Electric Field Gradients

In order to determine V_{zz} and η separately, one has to complement the NQR data by measuring the Cu NMR spectrum. The result for “1-2-4” in an external field of 4.7 T at 150 K is shown in Figure 4 [9]. The spectrum is a superposition of a quadrupolar second-order powder pattern [16] of the central transition $m = +1/2 \leftrightarrow -1/2$ and a frequency shift (Knight shift) to higher frequencies, which is proportional to the external magnetic field. The “peaks” and “shoulders” in the spectrum which correspond to singularities and discontinuities, respectively, in the Cu line shape distribution function can be connected with the quadrupole coupling constant $C = eQV_{zz}/h$ and the asymmetry parameter η by direct diagonalization of the Hamiltonian [17]. The Knight shift is defined as $\Delta B/B_0$, where ΔB is the average static field produced by particles of a Fermi liquid in an external magnetic field B_0 . K is a tensor since the Knight shift is related to the electronic susceptibility. The components of K can be determined from special orientations. For the evaluation of the EFG and the Knight shift the spectra of both Cu isotopes were used.

In Table 1 we have summarized the results for “1-2-4” [9] together with Knight shift data for “1-2-3-7”

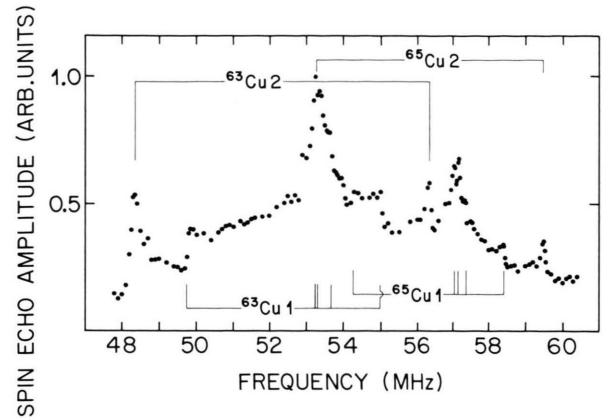


Fig. 4. NMR powder spectrum of the copper isotopes ^{63}Cu and ^{65}Cu for Cu1 and Cu2 sites in $\text{YBa}_2\text{Cu}_4\text{O}_8$ at 150 K. The vertical lines point to singularities in the frequency distribution (from [9]).

Table 1. Quadrupole coupling constant C , asymmetry parameter η and Knight shift components K_i at the ^{63}Cu sites in Y-Ba-Cu-O compounds. All K values are in units of percent (from Ref. [9]).

Cu1	Cu2
$\text{YBa}_2\text{Cu}_3\text{O}_7$ powder (reanalysis of data of Ref. [6], 300 K)	
$C = 38.9 \pm 0.5$ MHz	$C = 62.40 \pm 0.05$ MHz
$\eta = 0.95 \pm 0.05$	$\eta = 0.04 \pm 0.04$
$K_x = 0.6 \pm 0.2$	$K_{x,y} = 0.5 \pm 0.2$
$K_y = 0.5 \pm 0.2$	
$K_z = 1.5 \pm 0.4 (=K_a)$	$K_z = 1.2 \pm 0.4 (=K_c)$
$\text{YBa}_2\text{Cu}_3\text{O}_7$ aligned powder (Ref. [18], 100 K)	
$K_a = 1.338 \pm 0.015$	$K_{a,b} = 0.607 \pm 0.01$
$K_b = 0.607 \pm 0.015$	
$K_c = 0.600 \pm 0.01$	$K_c = 1.269 \pm 0.005$
$\text{YBa}_2\text{Cu}_4\text{O}_8$ (Ref. [9], 150 K)	
$C = 36.0 \pm 0.4$ MHz	$C = 59.44 \pm 0.04$ MHz
$\eta = 0.85 \pm 0.05$	$\eta = 0.01 \pm 0.01$
$K_x = 0.3 \pm 0.1$	$K_{x,y} = 0.4 \pm 0.1$
$K_y = 0.2 \pm 0.1$	
$K_z = 1.2 \pm 0.1 (=K_a)$	$K_z = 1.6 \pm 0.2 (=K_c)$

obtained by Takigawa et al. [18] for aligned powder. In addition, we have given the result of a reanalysis of our old data for “1-2-3-7” powder [6], now taking into account the anisotropy of the Knight shift. Our original analysis was based on an averaged Knight shift. Considering the errors, the “new” Knight shift data are in good agreement with those of Takigawa et al. [18]. We also like to point out that the new analysis has reduced $\eta(\text{Cu2})$ to 0.04 ± 0.04 , being now in agreement with single crystal data [19].

The similarity of the two structures shows up in small differences between corresponding parameters of the EFG tensors. The coupling constants C at both sites are slightly smaller in “1-2-4”. The nearly axial symmetry of the EFG at the Cu2 site [$\eta(\text{Cu2})$ being close to zero] in both compounds reflects the small deviation of this site from tetragonal symmetry. On the other hand, the large difference of the values of η for the Cu1 and Cu2 sites in both compounds is striking. A value of η close to 1 must reflect the peculiar electronic structure at the Cu1 site. Although the values for $\eta(\text{Cu1})$ in both structures overlap within the experimental errors, we believe that their difference is significant and demonstrates a reduction in asymmetry which might arise from the structural changes in “1-2-4” introduced by the second copper chain.

How can the EFG's be related to charge distributions and the electronic structure of the respective compound? Among others, one motivation for measuring the dependence of the NQR frequencies on both temperature and pressure was to have as much experimental information on the EFG as possible in order to put constraints on proposed calculations.

The simplest calculation of the EFG is by means of the point-charge model. The EFG at the nuclear site is determined by two contributions: one arises from the point charges on neighboring ions, the second from incomplete electronic shells of the ion under consideration (valence contribution). Thus the total EFG may be written as

$$V_{zz} = (1 - \gamma_\infty) V_{zz}^0 + (1 - R)(V_{zz})_{\text{val}}. \quad (4)$$

Here, V_{zz}^0 and $(V_{zz})_{\text{val}}$ are the EFG produced by neighboring ions and incomplete shells, respectively, and γ_∞ and R are the respective Sternheimer factors. A temperature and pressure behavior of ν_Q similar to that for Cu1 in “1-2-3-6” (see Fig. 3a) was observed for the *monovalent* Cu in Cu_2O [20], where the valence contribution in (4) vanishes. For the evaluation of V_{zz} at the Cu1 site [14] we have used the following charges: Y^{+3} , Ba^{+2} , Cu1^{+1} , Cu2^{+2} and -2 for all oxygen ions. We have taken the experimental Cu^{+1} Sternheimer anti-shielding factor $\gamma_\infty = -5.5$ from Cu_2O together with the ^{63}Cu electric quadrupole moment $Q = -0.211 \times 10^{-28} \text{ m}^2$. This yields for Cu1 $\nu_Q = 31.0 \text{ MHz}$, which is in excellent agreement with the 29.9 MHz experimental value.

In calculating the pressure dependence of $\nu_Q(\text{Cu1})$ in “1-2-3-6” we have assumed that the structure remains tetragonal and that the lattice constants change

similarly as in “1-2-3-7”, where data are available. It turned out that ν_Q is very sensitive to the coordinates of the neighboring O1 ion on the c axis. Allowing for a small variation of these coordinates within their experimental uncertainties resulted in a good prediction of the pressure variation of ν_Q . We thus conclude that the point charge model is adequate for the EFG calculation at the Cu1^{+1} site in “1-2-3-6”.

In case of Cu2^{+2} in “1-2-3-6” there is a valence contribution which is proportional to the expectation value $\langle r^{-3} \rangle$ of the valence orbitals. Since this value is not calculable with satisfactory precision we have turned around the calculation: from the experimental value for ν_Q of Cu2 [21] and the calculated lattice EFG the *valence* EFG could be extracted. This way we got 80 MHz for the valence quadrupole coupling constant [13].

Considering now the “1-2-3-7” data, one has to explain the extreme asymmetry of the EFG at the Cu1 site and why $\nu_Q(T)$ and $\nu_Q(P)$ of Cu1 are completely different from the corresponding values in “1-2-3-6”. To restrict the possibilities of the charge distribution, we allowed variation of the oxygen's and Cu1 charges only but kept Y^{+3} , Ba^{+2} and Cu2^{+2} constant (as before). Furthermore, we applied again the experimental $\gamma_\infty = -5.5$. In case of the Cu^{+2} valence contributions, a value was used that did not deviate more than 10% from the value we had obtained in “1-2-3-6”. A good overall agreement with the experimental data for both Cu1 and Cu2 has been achieved by choosing the following charges: $+2$ for Cu1, -1.3 for the chain oxygen O4, and -1.95 for all other oxygens [13]. Without having the charge of O4 quite different from -2 one cannot account for the high asymmetry of the Cu1 EFG.

However, in contrast to the “1-2-3-6” compound, for “1-2-3-7” it is not possible to describe with the same set of charges both the temperature and pressure dependence of the NQR frequencies *and* the magnitude of the EFG at both Cu sites. This demonstrates that in general the point charge model is not adequate. One can improve the model by taking into account the large oxygen polarizability in a self-consistent way; in ionic crystals these models work quite successfully. We have not pursued this way any further since a quantum mechanical *ab initio* calculation of the EFG's in “1-2-3-6” and “1-2-3-7” has just been published by Ambrosch-Axel et al. [22].

These authors use a method that is based on full potential linearized augmented plane wave calcula-

tions. Good agreement with experimental data is found for Cu1 in both compounds although the Cu1 asymmetry parameter in “1-2-3-7” is only 0.8. For the Cu2 sites in “1-2-3-7” the magnitude of the EFG is only half the experimental value. For both Cu sites in “1-2-3-7” the sum of the partial valence-charges amounts to a total Cu charge +1.93, which comes close to our value determined by the point charge model. The distribution of the charges over the 3d orbitals is crucial. A small transfer of 0.07 electrons from $d_{x^2-y^2}$ to d_{z^2} symmetry is sufficient to achieve agreement between experimental and theoretical Cu2 EFG values. It remains to be seen how these ab initio calculations can reproduce the subtle but distinct differences that exist for the pressure and temperature variations of ν_{Q} of different sites.

5. Knight Shift

As can be seen from Table 1, the Knight shifts in both structures are much larger than the value 0.23% found in metallic copper. The parameters K_i ($i=x, y, z$) denote the principal components of the Knight shift tensor K . We have assumed that its principal axes coincides with those of the respective EFG tensor. The assignment of a component to a specific crystallographic axis is based on symmetry arguments.

When going from “1-2-3” to “1-2-4”, we note that all components of $K(\text{Cu1})$ decrease although the K_z values are equal within the error bars. The K_x and K_y components in “1-2-4” are about two to three times smaller than the corresponding values in “1-2-3”. For the Cu2 site, on the other hand, the K_z is larger in “1-2-4” than in “1-2-3” while $K_{x,y}$ (just as for Cu1) is again smaller in “1-2-4” than in “1-2-3”.

Generally, for a transition element the Knight shift contains a spin and an orbital contribution. For a separate estimate of these parts one needs data from the superconducting phase. For “1-2-3” [18] it turned out that the orbital part at Cu2 is very anisotropic. Using aligned powder we are going to perform similar measurements in “1-2-4” and to search whether differences between both structures are present and how they can be related to differences in valency and structure.

6. Relaxation Times

Measurements of the spin-lattice and spin-spin relaxation times (T_1 and T_2 , respectively) microscopi-

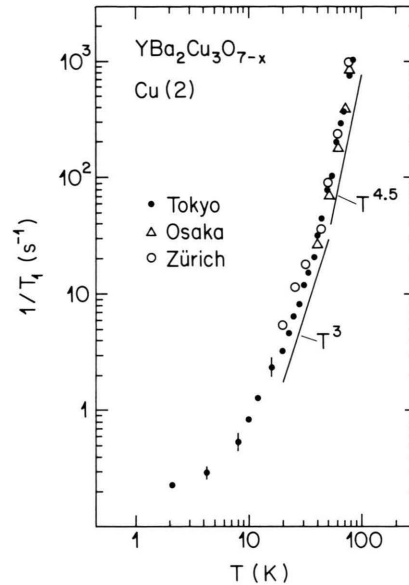


Fig. 5. Summary of Cu2 relaxation rates in $\text{YBa}_2\text{Cu}_3\text{O}_7$. Full circles: [24], triangles: [23], open circles: [6].

cally probe the spin dynamics at the nuclear sites. One of the important questions is whether the superconducting order parameter is of Bardeen-Cooper-Schrieffer (BCS) nature as in conventional superconductors. If the rates in the superconducting phase could be described within the *traditional* framework of the BCS theory of NMR relaxation [1], they should obey the function $\exp(-\Delta/k_B T)$, where 2Δ is the size of the energy gap. In addition, one would expect an increase of the rates followed by a peak just below T_c . Such an enhancement is generally attributed to “piling up” of the BCS density of states at the gap edge.

We have determined by NQR T_1 and T_2 in both the “1-2-3” [6, 7, 8] and the “1-2-4” structure [9] over a wide range of temperatures and partly at elevated pressure [13] for all sites and in all phases. In “1-2-3-7” and above T_c , T_1 for Cu1 and Cu2 is independent of pressure up to 0.6 GPa, i.e. the high frequency fluctuations giving rise to relaxation are not affected by pressure. We discuss some results concerning the T_1 temperature dependence in “1-2-3-7” and “1-2-4”.

Neither in “1-2-3-7” nor in “1-2-4” we have detected a peak just below T_c ; no exponential decrease of the rates present over a *wide range* of temperatures was found. On the contrary, in “1-2-3” below T_c , the Cu2 relaxation rates could be fitted by a power law $1/T_1 \propto T^n$ with $n \approx 3$ to 5. Figure 5 demonstrates the good agreement of our data with previous measure-

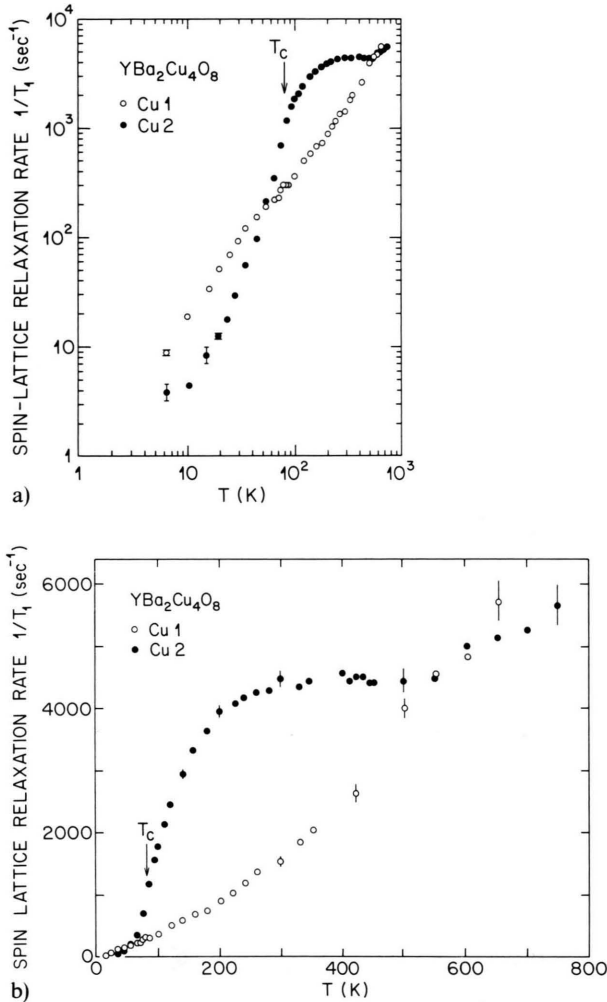


Fig. 6. Temperature dependence of the spin-lattice relaxation rate of ^{63}Cu for Cu1 and Cu2 sites in $\text{YBa}_2\text{Cu}_4\text{O}_8$: Fig. 6a: log-log plot, Fig. 6b: linear plot (from [9]).

ments of Kitaoka et al. [23] and Imai et al. [24]. Such a behavior, which has been observed before in heavy fermion and organic superconductors, is expected for conductors with an anisotropic energy gap that is zero on points or lines of the Fermi surface.

Figures 6a and 6b [9] show the relaxation rates for “1-2-4” in two different presentations. It is obvious, that a power law fit is only possible for the Cu1 rates with a low exponent $n \approx 1.35$ valid for the whole superconducting phase. On the other hand, the Cu2 rates in “1-2-4” can be fitted quite well (except for the 6 K point) by $1/T_1 \propto \exp(\sqrt{T/T_0})$ with $T_0 = 1.14$ K. Imai et al. [24] have described such a fit already for the

Cu1 and Cu2 data in “1-2-3” with values $T_0 = 0.76$ K and 2.0 K for Cu2 and Cu1, respectively, which are surprisingly close to our result. The origin of the mechanism leading to such a relaxation behavior seems to be still unknown.

One of the striking differences between “1-2-3-7” and “1-2-4” is the “smooth” transition of the Cu2 relaxation rate from the normal to the superconducting state in “1-2-4” without any discontinuity or abrupt change in the slope (see Figure 6). On the other hand: the Cu2 rates at T_c in “1-2-3” and “1-2-4” are nearly identical!

Considering now the normal phase of “1-2-4” (Fig. 6b), we first note that the Cu1 relaxation rate can be fitted by

$$1/T_1 = aT + bT^2, \quad (5)$$

where $a = 2.61 (\text{s K})^{-1}$ and $b = 0.0095 \text{ s}^{-1} \text{ K}^{-2}$. We have reanalysed our Cu1 relaxation data in “1-2-3-7” [6] and found that they also can be described by (5) with $a = 17 (\text{s K})^{-1}$ and $b = 0.043 \text{ s}^{-1} \text{ K}^{-2}$. A linear dependence of the rate on temperature is expected if the nuclei interact with the hyperfine fields of a Fermi liquid. The quadratic term bT^2 in (5) is attributed to quadrupolar interaction of the Cu1 nuclei with phonons.

It seems that the Cu2 rates in “1-2-4” can also be described by a linear term, however, only above 550 K where we find $1/T_1 = AT$ with $A = 7.8 (\text{s K})^{-1}$. Between T_c and 550 K the rate is enhanced with respect to this linear dependence. We have suggested [9] to explain this behavior in terms of a model recently proposed by Monien et al. [25], which goes as follows. Itinerant quasiparticles formed by hybridization of local Cu^{2+} moments and oxygen holes couple with Cu nuclei. For the Cu2 system there is a strong interaction between the quasiparticles represented by the averaged effective interaction constant \bar{J} . For the Cu1 system these interactions are supposed to be absent. These interactions lead to an enhancement of the correlation time τ representing the duration of a magnetic fluctuation, by a factor $(1 - N(0)\bar{J})^{-2}$ where $N(0)$ is the quasiparticle density of states. The increase of the rate at 550 K then could reflect the breakdown of the interaction between the quasiparticles. Above 550 K the relaxation rate then depends linearly on temperature as expected for relaxation due to non-interacting quasiparticles. This interpretation is favored by the fact that the ratio of the parameters A and a (from (5)) is about equal to the square of the ratio of the corre-

sponding Knight shift components $K_{x,y}$ for Cu2 and Cu1. We like to point out that a similar behavior of the Cu2 relaxation rate in "1-2-3-7" might have escaped experimental detection because the thermal instability of the compound forbids experiments at higher temperatures.

Acknowledgement

Valuable and stimulating discussions with the members of our NMR group, Dr. M. Mali, Dr. J. Roos, Katharina Müller, H. Schiefer, and H. Zimmermann, are gratefully acknowledged.

- [1] For instance: D. E. MacLaughlin, *Solid State Phys.* **31**, 1 (1976).
- [2] See for instance: Proceedings of the Intern. Conf. on High Temperature Superconductors and Materials and Mechanisms of Superconductivity (M²S-HTSC), *Physica C* **153–155** (1988).
- [3] J. Karpinski, E. Kaldis, E. Jilek, S. Rusiecki, and B. Bucher, *Nature London* **336**, 660 (1988).
- [4] P. Marsh, R. M. Fleming, M. L. Mandich, A. M. De Santo, J. Kwo, M. Hong, and L. J. Martinez-Miranda, *Nature London* **335**, 141 (1988).
- [5] P. Fischer, J. Karpinski, E. Kaldis, E. Jilek, and S. Rusiecki, *Solid State Commun.* **69**, 531 (1989).
- [6] M. Mali, D. Brinkmann, L. Pauli, J. Roos, H. Zimmermann, and J. Hulliger, *Phys. Lett. A* **124**, 112 (1987).
- [7] M. Mali, J. Roos, and D. Brinkmann, Ref. [2], p. 737.
- [8] D. Brinkmann, Ref. [2], p. 75.
- [9] H. Zimmermann, M. Mali, D. Brinkmann, J. Karpinski, E. Kaldis, and S. Rusiecki, *Physica C* **159**, 681 (1989).
- [10] H. Schiefer, M. Mali, J. Roos, H. Zimmermann, D. Brinkmann, E. Kaldis, and J. Karpinski, *Physica C*, to be published.
- [11] E. Kaldis, P. Fischer, A. W. Hewat, E. A. Hewat, J. Karpinski, and S. Rusiecki, *Physica C* **159**, 668 (1989).
- [12] M. Mali, J. Roos, and D. Brinkmann, unpublished data.
- [13] Katharina Müller, M. Mali, J. Roos, and D. Brinkmann, *Physica C*, to be published.
- [14] R. L. Cava, J. J. Krajewski, W. P. Peck Jr., B. Batlogg, L. W. Rupp Jr., R. M. Fleming, A. C. W. P. James, and P. Marsh, *Nature London* **338**, 328 (1989).
- [15] Katharina Müller, Diploma Thesis, University of Zürich (1989).
- [16] M. H. Cohen and F. Reif, *Solid States Physics* **5**, 321 (1957).
- [17] R. B. Creel, *J. Magn. Reson.* **52**, 515 (1983).
- [18] M. Takigawa, P. C. Hammel, R. H. Heffner, Z. Fisk, J. L. Smith, and R. B. Schwarz, *Phys. Rev. B* **39**, 300 (1989).
- [19] C. H. Pennington, D. J. Durand, D. B. Zax, C. P. Slichter, J. P. Rice, and D. M. Ginsberg, *Phys. Rev. B* **37**, 7944 (1988).
- [20] T. Kushida, G. B. Benedek, and N. Bloembergen, *Phys. Rev.* **104**, 1364 (1956).
- [21] H. Yasuoka, T. Shimizu, Y. Ueda, and K. Kosuge, *J. Phys. Soc. Japan* **57**, 2659 (1988).
- [22] C. Ambrosch-Draxl, P. Blaha, and K. Schwarz, *J. Phys. Cond. Matter*, in press (1989).
- [23] Y. Kitaoka, S. Hiramatsu, Y. Kohori, K. Ishida, T. Kondo, H. Shibai, K. Asayama, H. Takagi, S. Uchida, H. Iwabuchi, and S. Tanaka, *Physica C* **153–155**, 83 (1988).
- [24] T. Imai, T. Shimizu, H. Yasuoka, Y. Ueda, and K. Kosuge, *J. Phys. Soc. Japan* **57**, 2280 (1988).
- [25] H. Monien, D. Pines, and C. P. Slichter, preprint.